



EUROPEAN
COMMISSION

Community research

PEBS

(Contract Number: FP7 249681)

DELIVERABLE (D-N°: 2.2-9)

Thermal Characterisation of HE-E Buffer

Author(s):

Klaus Wieczorek, Rüdiger Miehe
with contributions of Benoit Garitte

Reporting period: 01/03/10 – 30/06/13

Date of issue of this report: 24/09/13

Start date of project: 01/03/10

Duration : 48 Months

Project co-funded by the European Commission under the Seventh Euratom Framework Programme for Nuclear Research & Training Activities (2007-2011)		
Dissemination Level		
PU	Public	PU
RE	Restricted to a group specified by the partners of the [acronym] project	
CO	Confidential, only for partners of the [acronym] project	

PEBS



Table of Contents

1	Introduction	1
2	Measurement techniques	3
2.1	Thermal parameters	3
2.2	Densities and water content	4
2.3	Retention curve (granular sand-bentonite mixture)	5
2.4	Permeability (granular sand-bentonite mixture)	5
3	Measurements on bentonite blocks	6
3.1	Sample preparation and nomenclature	6
3.2	Determination of thermal parameters	7
3.3	Results for bentonite blocks	8
3.3.1	Bulk density	8
3.3.2	Grain density	9
3.3.3	Water content	9
3.3.4	Thermal parameters	9
4	Measurements on granular sand-bentonite mixture	15
4.1	Sample preparation for measurement of thermal parameters	15
4.2	Determination of thermal parameters	19
4.2.1	Bulk density	19
4.2.2	Grain density	20
4.2.3	Water content	20
4.2.4	Thermal parameters at varying temperature	20
4.2.5	Thermal conductivity as a function of water content	23
4.3	Sample preparation and measurement of retention curve	24
4.4	Permeability of granular sand-bentonite	29
5	Measurements on granular bentonite	31
5.1	Sample preparation	32
5.2	Determination of thermal parameters	32

6	Conclusions and remaining work	36
7	References.....	38
8	List of figures	39
9	List of tables	41

1 Introduction

The heater experiment HE-E is performed in the frame of the EC project “Long-term performance of Engineered Barrier Systems” (PEBS) /PEB 10/ in a microtunnel in the Mont Terri rock laboratory in Switzerland. Two horizontal heaters are installed in two sections of the tunnel with different buffer types (Fig. 1.1)

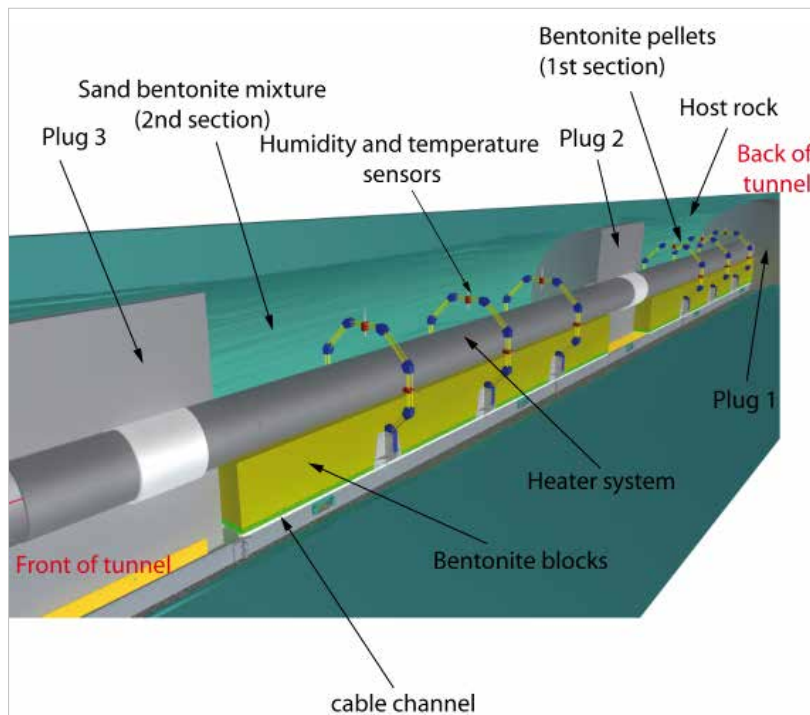


Fig. 1.1 Overview of the HE-E configuration

Three buffer materials are used in the experiment:

- The heater is placed on a foundation of highly compacted bentonite blocks in both sections.
- In one section, the remaining void is backfilled with granular bentonite material.
- In the second section, the backfill material is a mixture of 65 % sand and 35 % granular bentonite of the same grain spectrum.

The buffer materials are specified in the HE-E as-built report /TEO 12/.

In order to obtain data on the thermal parameters (thermal conductivity, thermal capacity, and thermal diffusivity) of these materials, respective tests on samples are performed at the

GRS laboratory in Braunschweig. For the tests a „Hot Disk Thermal Constants Analyser“ /HDT 07/ is used.

The schedule of the tests is determined by the needs of the modelling groups that perform numerical simulations of the HE-E.

- During the first years of heating, the buffer saturation will remain low, but the buffer temperature will increase rapidly. For interpretative modelling of this test phase, the thermal parameters at as-emplaced saturation and at ambient and elevated temperature are needed.
- At later times, the buffer will begin to re-saturate. For predictive calculations of later experiment stages, the dependence of the thermal parameters on saturation has to be quantified.

The measurements at low saturation and at ambient and elevated temperature were completed for the bentonite blocks and the sand-bentonite mixture and documented in the PEBS Deliverable D2.2-5 (“Measurement of Thermal Parameters of the HE-E Buffer Materials”) end of 2011 /WIE 11/.

In the meantime, more measurements have been performed. Dependence of thermal parameters of the sand-bentonite mixture on saturation has been established, although not yet for the whole saturation range. In addition to the measurement of thermal parameters, the retention curve and the permeability of the sand-bentonite were investigated, since no respective data were available, but needed for modelling.

All the results obtained to date are included in this deliverable D2.2-9, which has to be seen as an update of D2.2-5. Still, not all experimental work has been finished yet. The dependence of thermal parameters on saturation is still under investigation for the pure granular bentonite and, at high saturation, for the sand-bentonite. An update of this deliverable will be issued as soon as all the results are available.

2 Measurement techniques

For all three types of buffer materials – bentonite blocks, bentonite pellets, and granular sand-bentonite mixture – the thermal parameters and the related densities and water content have been determined.

In addition to these measurements, the lack of respective data for the sand-bentonite mixture required measurement of the retention curve and the permeability.

2.1 Thermal parameters

For the measurement of thermal parameters a heating sensor in the form of a double spiral consisting of a thin metal sheet insulated by a Kapton body is placed inside the investigated material. An electric current is led through the sensor which increases its temperature in a range between a fraction of one degree and several degrees Celsius. The alteration of the sensor's electric resistivity is a measure for the thermal parameters of the material. The sensor thus has a combined function of providing the heat source and the dynamic measurement. The principle measurement configuration is shown in Fig. 2.1. Different sensor sizes are available for measurement in different materials (Fig. 2.2).

The analyser outputs the thermal conductivity, thermal capacity, and thermal diffusivity of the sample material. It has to be noted that thermal capacity is given as a volumetric specific heat (in MJ/(m³*K)). In order to obtain the thermal capacity per mass the output value has to be divided by the bulk density of the sample.

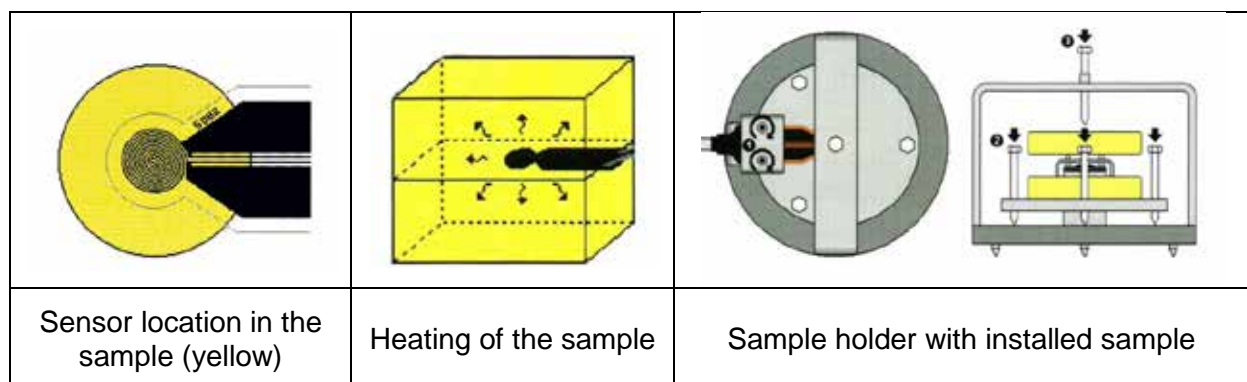


Fig. 2.1 Principle measurement configuration /HDT 07/



Fig. 2.2 Sensors for the Hotdisk analyser

For performing measurements of the thermal parameters at elevated temperature, the sample/sensor combination can be placed in a drying oven with fittings for the cables. The sample is left in the oven for several hours to ensure the oven temperature has been reached throughout the sample; then the measurement is performed with the sample inside the oven.

The sample volume that is actually affected by the measurement is rather small. Therefore, it is essential to provide a good coupling between the sample and the measuring probe; otherwise, heat conduction at the contact will be inhibited and the thermal conductivity may be underestimated.

2.2 Densities and water content

Besides the thermal parameters, bulk density, grain density and water content were determined. Bulk density was calculated from sample geometry and mass. Grain density was measured using a helium pycnometer. Water content was determined by weighing before and after drying at 105 °C.

2.3 Retention curve (granular sand-bentonite mixture)

For determination of the retention curve samples of sand-bentonite mixture were re-saturated in exsiccators containing different salt solutions in order to obtain different relative humidities in the atmosphere. The relative air humidity was measured. From the humidity the suction was calculated. The saturation of each sample was afterwards determined by oven-drying at 105 °C.

2.4 Permeability (granular sand-bentonite mixture)

For permeability measurement a sand-bentonite sample with original water content was emplaced in a cylindrical cell. Gas injection tests were performed at five pressure steps. Afterwards, the sample was re-saturated and the permeability of the saturated sample to water was determined by water injection testing.

3 Measurements on bentonite blocks

Two types of bentonite blocks are used in the HE-E: The upper blocks have a groove in which the heater is held (see Fig. 3.1). The lower blocks are simply brick-shaped. One block of each type was available for sampling and investigation of the thermal parameters.

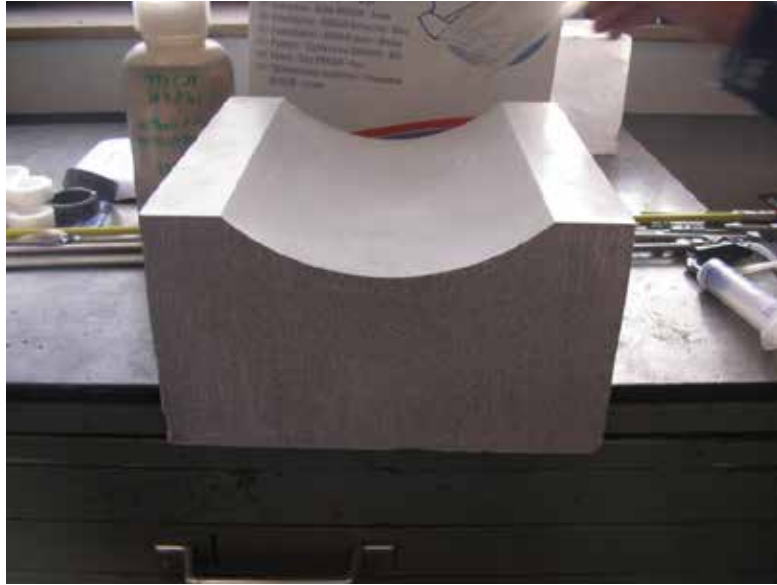


Fig. 3.1 Grooved upper bentonite block

3.1 Sample preparation and nomenclature

In order to check whether there are differences between the centre and the near-surface zones of the blocks, samples were taken from both blocks both from the centre and the near-surface. The samples from the block centre were named with the letters STA (for the upper block) or STU (for the lower block) and a number from 1 to 6. The samples 1 through 4 of each block were heated in steps from 20 °C to 105 °C in the state as delivered and the thermal parameters were determined at each step. The sample 5 and 6 were first dried at 105 °C (following DIN 18121) and the temperature dependence of the thermal parameters was measured on the dried samples. In order to obtain the moisture loss due to heating an additional reference sample for determining moisture content was used in each case. The change of bulk density of the sample due to heating was used to recalculate the mass-related specific heat of the samples (see Section 2).

The samples were sawed from the blocks. The sawdust obtained was used for determining the grain density. The dimensions of all samples are 60 mm by 60 mm by 30 mm (Fig. 3.2). For the measurements two single samples (e.g., STU1 and STU2) were put together with the sensor in between. Thus, the considered sample pairs had a size of 60 mm by 60 mm by 60 mm.



Fig. 3.2 Sample pair STU1/STU2

3.2 Determination of thermal parameters

For the measurement the sensor is placed between the two single samples of one pair. Sensor coupling to the sample is ensured by use of a clamping device (Fig. 3.3). The tests are performed while the compound sample (sample pair with sensor) is placed in a drying oven with fittings for the cables. At each of the temperature steps of 20 °C, 40 °C, 60 °C, 80 °C und 105 °C a measurement is performed. A waiting time between the measurements is needed to ensure that a constant temperature has been reached in the sample. This time was set to approximately 7 h per step.



Fig. 3.3 Sample pair in the drying oven (the clamping device is used to assure coupling of sensor to the bentonite)

3.3 Results for bentonite blocks

3.3.1 Bulk density

The density values show a variation depending on block and sampling position. Close to the block surface, the samples from both blocks show density values of 2350 kg/m³ to 2450 kg/m³ (bulk density) and 2100 kg/m³ to 2190 kg/m³ (dry density), respectively. In the center of the blocks, 2060 kg/m³ bulk density (1840 kg/m³ dry density) were measured on the samples from the lower block, the values for the upper block of 2030 kg/m³ to 2070 kg/m³ bulk density (1830 kg/m³ to 1850 kg/m³ dry density) were comparable. These results compare well with measurements of ETH Zürich which are published in the HE-E as-built report /TEO 12/. ETH found a macroscopic density of 2080 kg/m³. After sampling from the blocks at ETH, however, somewhat smaller densities were found. This was explained by ETH by relaxation and drying between production and lab analysis. Indeed, the water content measured by ETH was lower than the values measured by GRS (see Section 3.3.3).

3.3.2 Grain density

Grain density was measured to be 2695.8 kg/m³ for the dry material, which compares well to ETH measurements of 2699 kg/m³. Earlier measurements resulting in lower values were found to have been caused by an instrument defect.

3.3.3 Water content

The water content of the different samples was very homogeneous: On the block surface, always 11.88 % were measured. Inside both blocks, values of 11.7 % to 11.83 % were obtained.

The water content measured by ETH ranged between 9.3 % and 11.6 %, with an average of 10.34 % /TEO 12/. This is somewhat lower and was explained by ETH by some drying between sample production and analysis (see also Section 3.3.1 on density). The water content of the sawdust samples for grain density determination at GRS was lower (5.1 % to 6.2 %), too. This is a consequence of the sawing procedure which led to drying.

3.3.4 Thermal parameters

In the Tables 3.1, 3.2, and 3.3 the measurement results for thermal conductivity, thermal diffusivity, and specific heat for the different temperature steps are given, together with bulk density and (remaining) water content. Tables 3.1 and 3.2 show the results for the upper and low block (as delivered), respectively. Note that the water content of the samples is reducing with each temperature step. Table 3.3 summarizes the respective results for samples from both blocks which were dried before the measurements.

The measurement results on thermal conductivity, thermal diffusivity, and specific heat with the different samples are compiled in the Figures 3.4 – 3.7.

Thermal conductivity (Fig. 3.4) of the as-delivered samples shows a slight decrease with temperature which can be attributed to the water loss during heating of the sample (see Tab. 3.1 and 3.2). For the previously dried samples this behaviour is not observed. It can be deduced that the thermal conductivity of the solid phase is independent of temperature in the considered temperature range. Variations of the thermal conductivity in the as-delivered

samples are thus exclusively related to replacement of the water phase in the pores by air (air having a lower thermal conductivity than water).

Tab. 3.1 Thermal parameters of the upper block, as delivered

Sample	Density	Thermal Conductivity	Thermal Diffusivity	Specific Heat	Temperature	Remaining Water Content
	ρ	K	K	c	T	w_r
	kg/m ³	W/(m*K)	mm ² /s	MJ/(kg*K)	°C	%
STA1 / STA2	2052	1.114	0.422	1.29*10 ⁻³	20°C	11.51
STA1 / STA2	2014	1.036	0.280	1.84*10 ⁻³	40°C	9.44
STA1 / STA2	1946	1.050	0.280	1.93*10 ⁻³	60°C	6.00
STA1 / STA2	1921	0.921	0.200	2.40*10 ⁻³	80°C	4.69
STA1 / STA2	1888	0.908	0.189	2.54*10 ⁻³	105°C	2.52
STA3 / STA4	2030	1.086	0.412	1.30*10 ⁻³	20°C	11.42
STA3 / STA4	1991	1.057	0.366	1.45*10 ⁻³	40°C	9.43
STA3 / STA4	1930	1.076	0.344	1.62*10 ⁻³	60°C	5.97
STA3 / STA4	1906	1.129	0.378	1.57*10 ⁻³	80°C	4.67
STA3 / STA4	1866	0.942	0.271	1.86*10 ⁻³	105°C	2.42

Tab. 3.2 Thermal parameters of the lower block, as delivered

Sample	Density	Thermal Conductivity	Thermal Diffusivity	Specific Heat	Temperature	Remaining Water Content
	ρ	K	K	c	T	w_r
	kg/m ³	W/(m*K)	mm ² /s	MJ/(kg*K)	°C	%
STU1 / STU2	2064	1.326	0.612	1.05*10 ⁻³	20°C	11.77
STU1 / STU2	2029	1.033	0.334	1.52*10 ⁻³	40°C	9.69
STU1 / STU2	1959	1.069	0.358	1.53*10 ⁻³	60°C	6.09
STU1 / STU2	1933	1.044	0.335	1.61*10 ⁻³	80°C	4.72
STU1 / STU2	1892	1.024	0.369	1.47*10 ⁻³	105°C	2.47
STU3 / STU4	2044	1.091	0.300	1.78*10 ⁻³	20°C	11.65
STU3 / STU4	2023	0.981	0.238	2.04*10 ⁻³	40°C	9.68
STU3 / STU4	1958	1.001	0.249	2.05*10 ⁻³	60°C	5.06
STU3 / STU4	1933	0.990	0.242	2.11*10 ⁻³	80°C	4.67
STU3 / STU4	1891	0.965	0.247	2.07*10 ⁻³	105°C	2.39

Tab. 3.3 Thermal parameters of the upper and lower block samples after drying

Sample	Density	Thermal Conductivity	Thermal Diffusivity	Specific Heat	Temperature	Remaining Water Content
	ρ	K	K	c	T	w_r
	kg/m ³	W/(m*K)	mm ² /s	MJ/(kg*K)	°C	%
STU5 / STU6	2093	0.812	0.431	$9.00 \cdot 10^{-4}$	20°C	0.1
STU5 / STU6	1838	0.820	0.410	$1.09 \cdot 10^{-3}$	40°C	0.41
STU5 / STU6	1833	0.845	0.398	$1.16 \cdot 10^{-3}$	60°C	0.21
STU5 / STU6	1830	0.885	0.415	$1.17 \cdot 10^{-3}$	80°C	0.02
STU5 / STU6	1826	0.791	0.284	$1.53 \cdot 10^{-3}$	105°C	0.1
STA5 / STA6	2037	0.777	0.539	$7.07 \cdot 10^{-4}$	20°C	0.14
STA5 / STA6	1847	0.763	0.470	$8.78 \cdot 10^{-4}$	40°C	1.14
STA5 / STA6	1845	0.812	0.472	$9.33 \cdot 10^{-4}$	60°C	1.02
STA5 / STA6	1836	0.771	0.378	$1.11 \cdot 10^{-3}$	80°C	0.51
STA5 / STA6	1828	0.810	0.404	$1.10 \cdot 10^{-3}$	105°C	0.07

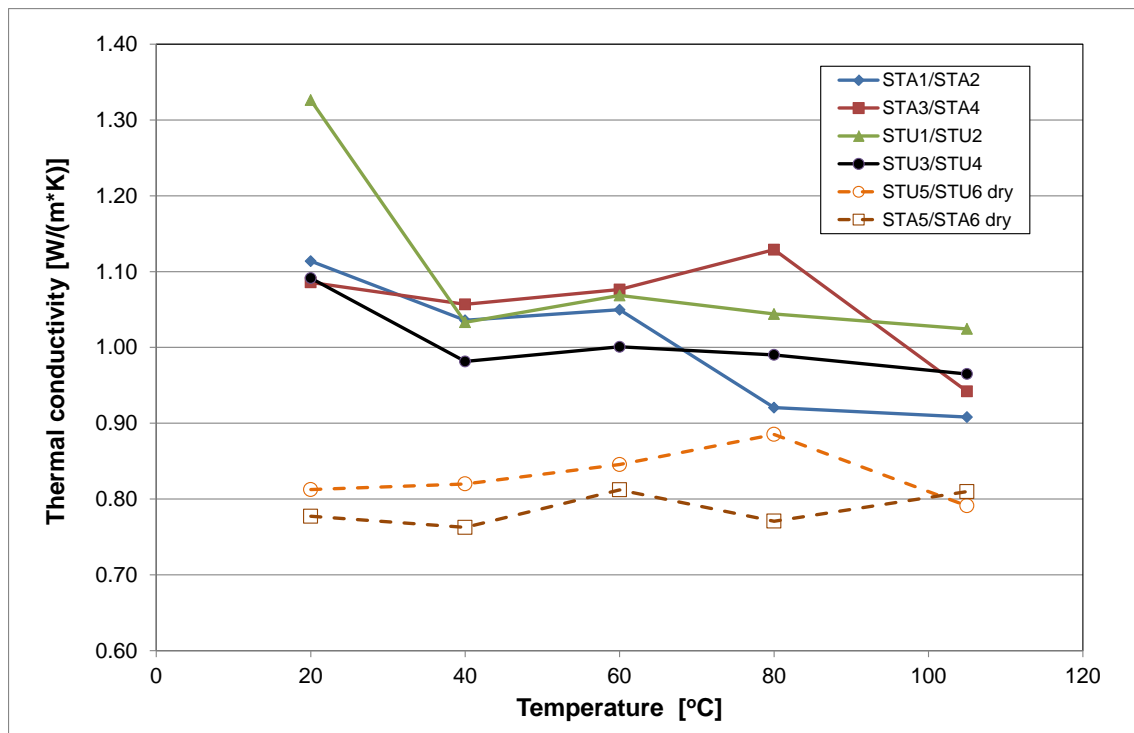


Fig. 3.4 Thermal conductivity of the different samples from the bentonite blocks as a function of temperature

The thermal conductivity of the as-delivered samples converges towards the dry sample value as temperature is increased. Nevertheless, the thermal conductivity values do not reach the low value measured in dry samples as the remaining water content of the as-delivered samples is still higher than that of the dried samples. This is illustrated in Fig. 3.5 where the results on thermal conductivity are plotted as a function of water content instead of temperature.

It can be expected that the thermal conductivity will increase further with higher water contents. Respective measurements will have to be performed to deduce a respective function. Significant temperature dependence, on the other hand, has not been found. For the as-delivered water content, a temperature-independent value of about 1.1 W/(m*K) seems to be a good approximation that could be used as starting value for the predictive calculations. During the first years of heating, no significant increase in saturation is expected. For simulating longer time spans when saturation increases, however, a saturation-dependent function for thermal conductivity will be needed.

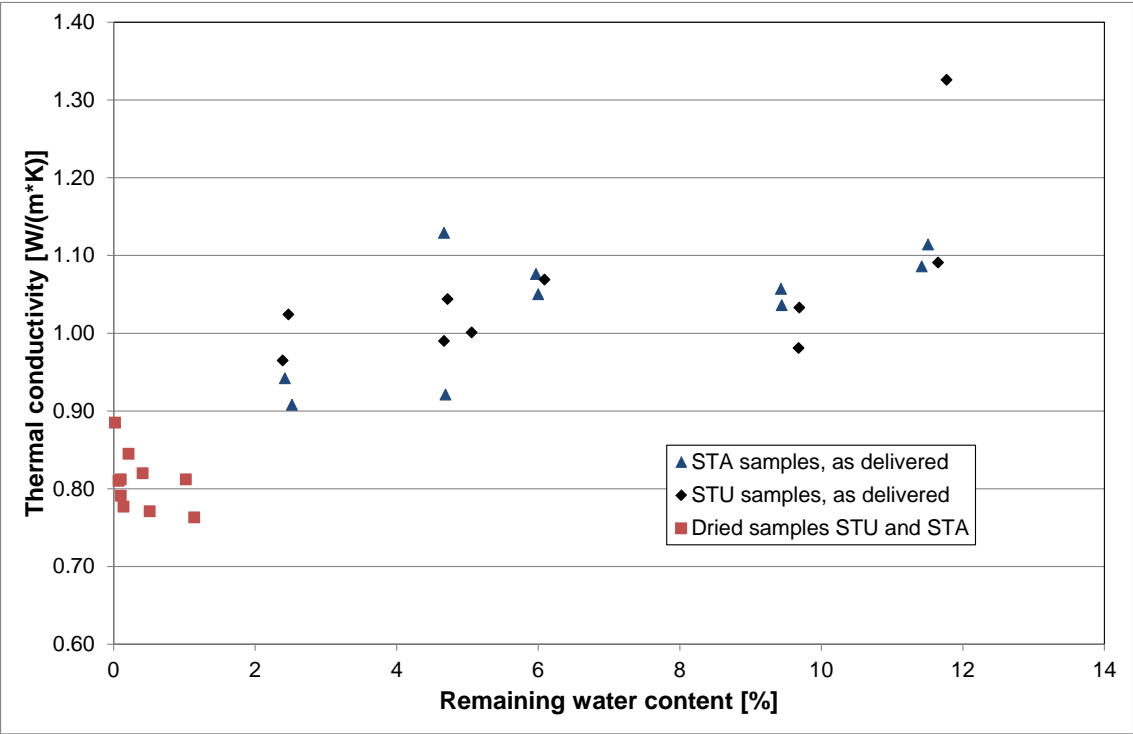


Fig. 3.5 Thermal conductivity of the different samples from the bentonite blocks as a function of water content

Thermal diffusivity (Fig. 3.6) shows a decrease with temperature for both the as-delivered and the dried samples. This is a consequence of the increase of specific heat (Fig. 3.7) of all samples with temperature – thermal diffusivity is not an independent parameter, but defined as ratio of thermal conductivity to the product of density and specific heat:

$$k = \frac{l}{r \times c}$$

Specific heat shows rather large variations between the as-delivered samples. The measured values for the dried samples are considerably lower, showing that water content seems to have a considerable influence on the specific heat. While the temperature effect on the results is visible, the variations between the individual as-delivered samples are much higher. Therefore, it seems reasonable to neglect the temperature dependence and assume a constant specific heat for a certain water content. A value of 1.8×10^{-3} MJ/(kg*K) seems appropriate for as-delivered water content in the temperature range covered in the HE-E. With increasing saturation, it can again be expected that specific heat will change, just as thermal conductivity does. Consequently, the dependence of specific heat on water content will have to be quantified.

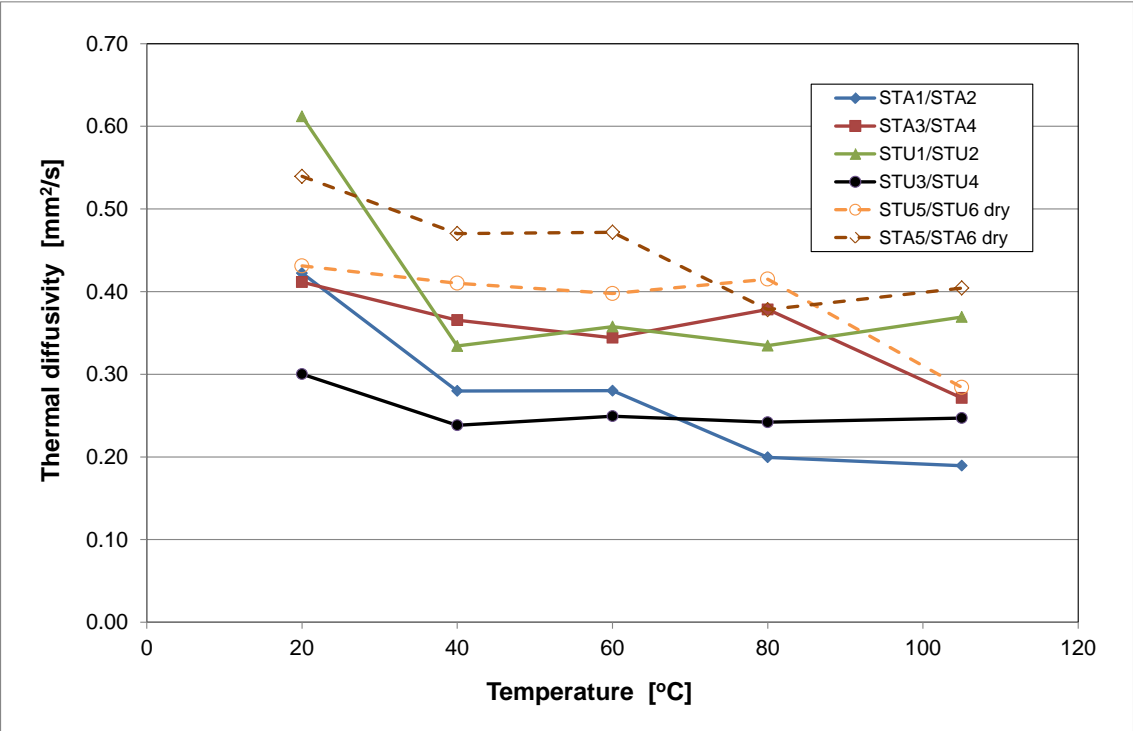


Fig. 3.6 Thermal diffusivity of the different samples from the bentonite blocks as a function of temperature

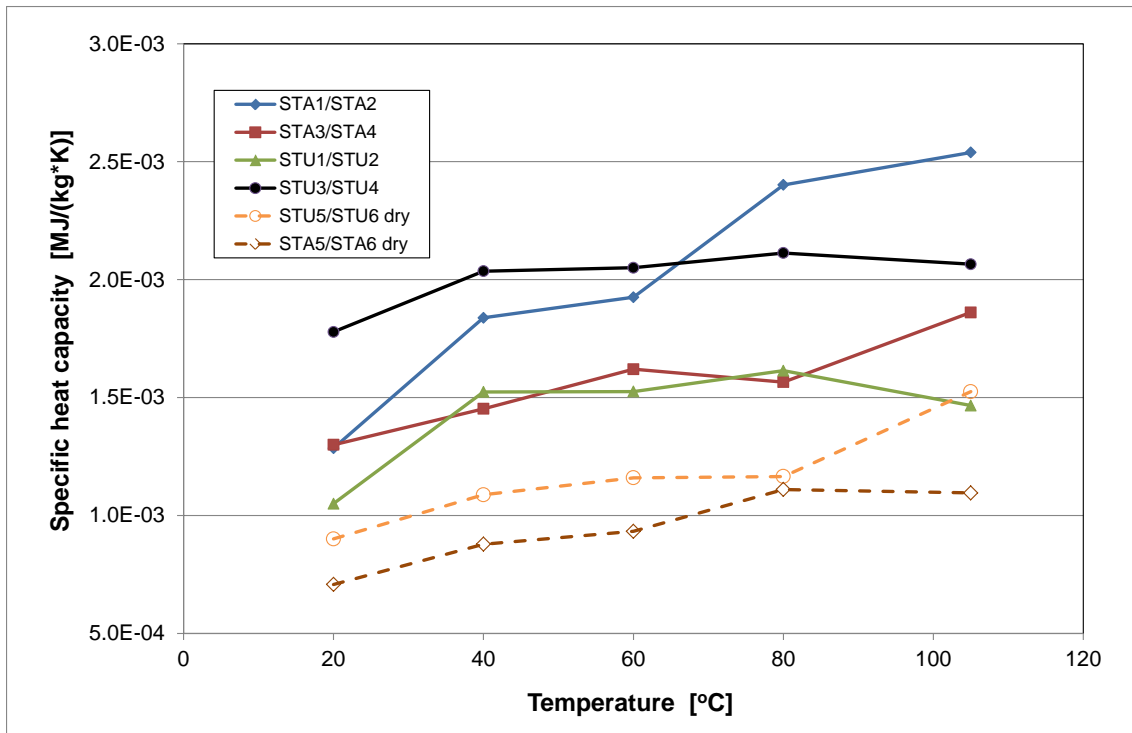


Fig. 3.7 Specific heat of the different samples from the bentonite blocks as a function of temperature

Thermal diffusivity should then be calculated from the employed values for thermal conductivity and specific heat – if needed at all in the model calculations.

4 Measurements on granular sand-bentonite mixture

The measurements were performed on samples consisting of a mixture of sand (65 wt.%) and granular sodium bentonite GELCLAY WH2 (35 wt.%) with an identical grain spectrum of 0.5 – 1.8 mm. For this granular material a special sample container had to be developed (see Section 4.1). The sample container, however, made it impossible to determine water content of the sample at each temperature step. Therefore, an individual sample of the as-delivered material was prepared for each temperature step between 20 °C and 105 °C. After the measurement of the thermal parameters, the water content was measured for each sample. Since evaporation is hindered by the sample container, it showed that all samples had approximately the same water content (in contrast to the bentonite blocks which had open surfaces for evaporation).

4.1 Sample preparation for measurement of thermal parameters

The sample container which had to be made for the measurements is shown in Fig. 4.1. The container was first filled with a sand-bentonite (SB) layer of 30 mm height which was compacted to a density of 1500 kg/m^3 , the density that was measured for the SB buffer emplaced in the HE-E (Fig. 4.2).



Fig. 4.1 Sample container for SB samples

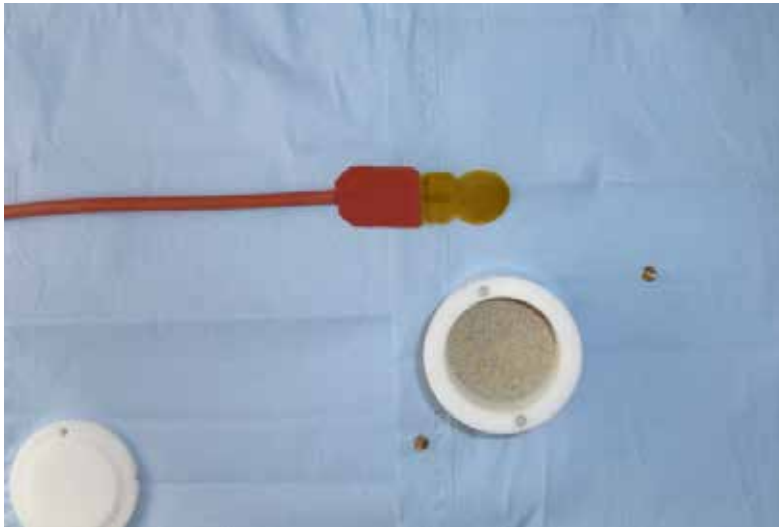


Fig. 4.2 Sample container with SB layer, in red: measurement sensor

Then, the sensor was inserted by a slot in the container side, so that it lay on top of the SB layer (Figs. 4.3 and 4.4).



Fig. 4.3 Inserting the sensor into the sample container



Fig. 4.4 Sensor and SB layer inside the sample container

Afterwards, a second layer of SB material was filled into the container and compacted (Figures 4.5 and 4.6).



Fig. 4.5 Emplacement of second SB layer into the sample container



Fig. 4.6 Filled sample container before closing

Finally, the filled sample container was closed with a lid and placed in the oven, which is equipped with lead-throughs for the connection cable (Fig. 4.7).



Fig. 4.7 Prepared sample in the oven

4.2 Determination of thermal parameters

Each of the samples with as-delivered water content was placed in the oven for six hours at the target temperature (20 °C, 40 °C, 60 °C, 80 °C und 105 °C); then the thermal parameters were measured. Afterwards, the sample was dried for the determination of water content.

For comparison, measurements were performed on samples of dried material as well. The dry samples were measured at the same temperature steps, but the same samples were used for the different steps, since no change in water content needed to be considered. The time for each step was one day. The samples were not removed from the container between the steps.

4.2.1 Bulk density

The bulk density of the samples from as-delivered material was quite homogeneous with values between 1517 kg/m³ and 1548 kg/m³ (see Tab. 4.1).

The density of the dried samples did not vary significantly. For the calculation of the specific heat a mean value of 1503 kg/m³ could be used (Tab. 4.2).

Tab. 4.1 Thermal parameters of the granular sand-bentonite buffer material at as-delivered water content

Sample	Density	Thermal Conductivity	Thermal Diffusivity	Specific Heat	Temperature	Water Content
	ρ	K	K	c	T	w _r
	kg/m ³	W/(m*K)	mm ² /s	MJ/(kg*K)	°C	%
sand/bentonite granulate (65/35)	1517	0.300	0.247	7.99*10 ⁻⁴	20°C	3.51
sand/ bentonite granulate (65/35)	1537	0.368	0.269	8.89*10 ⁻⁴	40°C	3.36
sand/ bentonite granulate (65/35)	1548	0.404	0.284	9.20*10 ⁻⁴	60°C	3.54
sand/ bentonite granulate (65/35)	1543	0.418	0.276	9.84*10 ⁻⁴	80°C	3.48
sand/ bentonite granulate (65/35)	1518	0.437	0.204	1.44*10 ⁻³	105°C	3.4

Tab. 4.2 Thermal parameters of the dried granular sand-bentonite buffer material

Sample	Density	Thermal Conductivity	Thermal Diffusivity	Specific Heat	Temperature	Water Content
	ρ	K	κ	c	T	w_r
	kg/m ³	W/(m*K)	mm ² /s	MJ/(kg*K)	°C	%
sand/bentonite granulate (65/35) dry	1503	0.297	0.2553	7.74*10 ⁻⁴	20°C	dry
sand/ bentonite granulate (65/35) dry	1503	0.3015	0.2587	7.75*10 ⁻⁴	40°C	dry
sand/ bentonite granulate (65/35) dry	1503	0.3061	0.2484	8.20*10 ⁻⁴	60°C	dry
sand/ bentonite granulate (65/35) dry	1503	0.3168	0.2449	8.61*10 ⁻⁴	80°C	dry
sand/ bentonite granulate (65/35) dry	1503	0.3253	0.2399	9.02*10 ⁻⁴	105°C	dry

4.2.2 Grain density

The grain density was determined on the dried material; the resulting value was 2546 kg/m³.

4.2.3 Water content

The water content of the individual samples did not show a great variation (Tab. 4.1) after the measurement at elevated temperature. The mean value was at 3.5 % and compares well with the original material. Obviously, evaporation from the sampling container was insignificant.

For the dried sample a slight increase to 0.06 % of water was observed after the measurement, which was a consequence of the sample taking up air humidity after removal from the oven.

4.2.4 Thermal parameters at varying temperature

The thermal conductivity of the samples with as-delivered water content is steadily rising with temperature (Tab. 4.1 and Fig. 4.8). Thermal conductivity of water rises with temperature, but the increase of the thermal conductivity measured in the samples cannot be attributed to that because of the small water content of the samples. In addition, the same trend, although less pronounced, can be seen for the dried samples (Tab. 4.2 and Fig. 4.8).

An explanation may be that the increased temperature in the confined sample leads to thermal stresses and a somewhat softer behaviour of the material (especially if some water is present). This may result in an improved coupling between the granular material and the sensor. Such a behaviour was not found for the bentonite blocks, because of their higher thermal conductivity (as a consequence of higher density and water content), better coupling from the beginning, and because of the fact that the blocks' thermal expansion is not restricted by a container. Because of the rather small sample dimensions and, in comparison, large contact surface coupling seems to be a major problem for this type of measurement, especially for granular material.

Thermal diffusivity and specific heat are shown in Figs. 4.9 and 4.10. Specific heat is again slightly increasing with temperature. The reason for the extreme value of the as-delivered sample at 105 °C is unclear. Otherwise, a value of $9 \cdot 10^{-4}$ MJ/(kg*K) seems appropriate for model calculations at as-delivered water content.

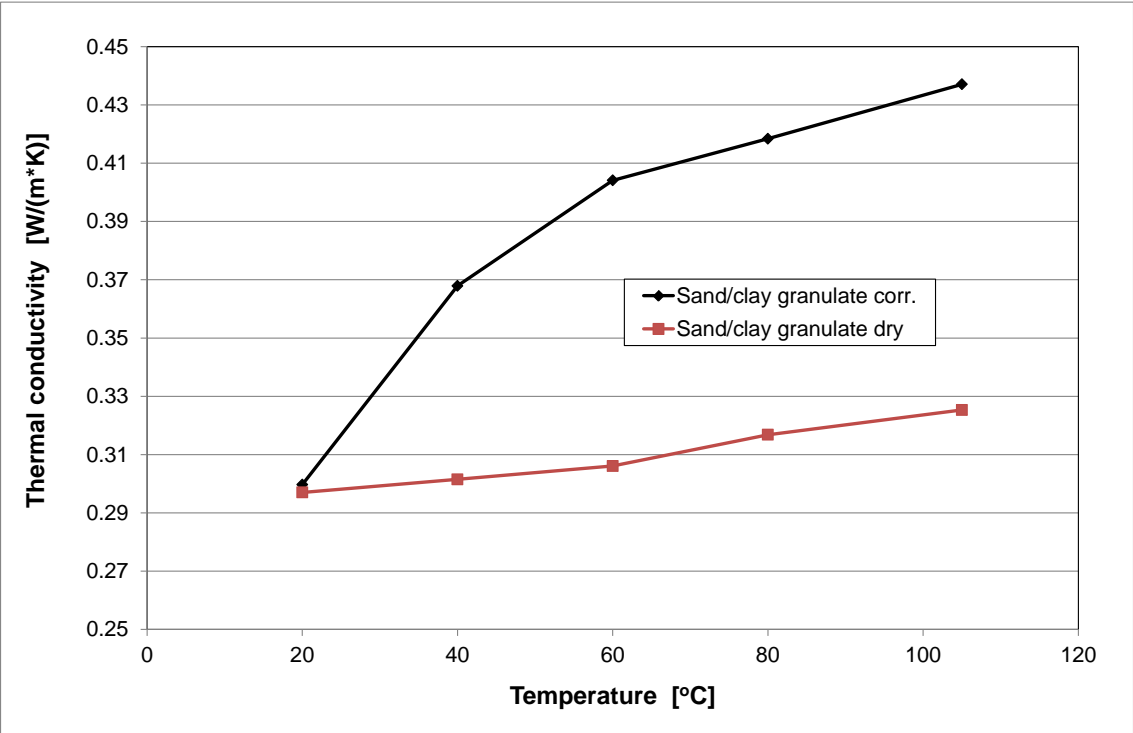


Fig. 4.8 Thermal conductivity of the dry (red) and as-delivered (black) SB samples as a function of temperature

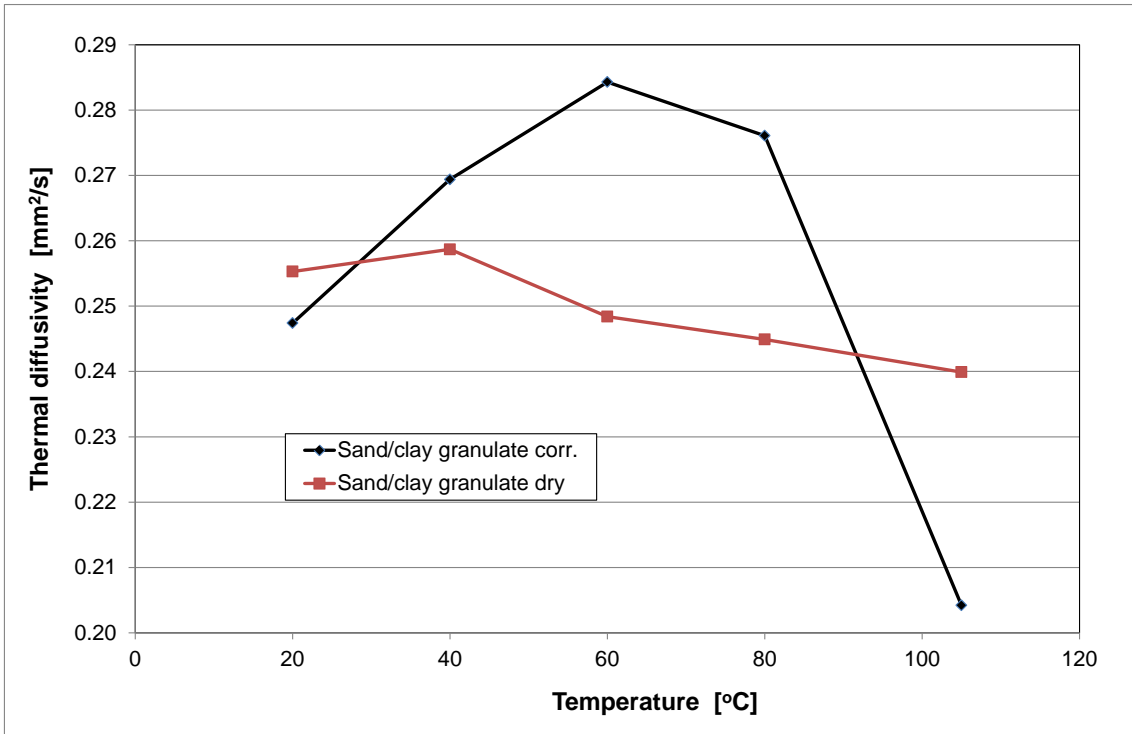


Fig. 4.9 Thermal diffusivity of the dry (red) and as-delivered (black) SB samples as a function of temperature

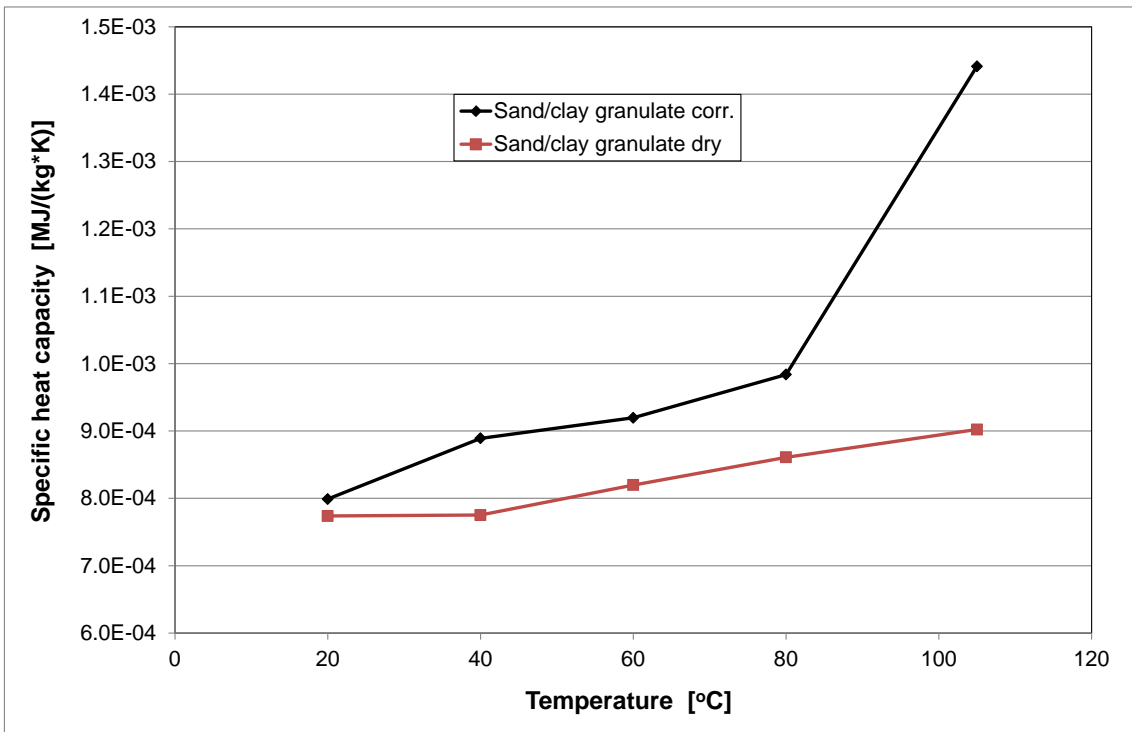


Fig. 4.10 Specific heat of the dry (red) and as-delivered (black) SB samples as a function of temperature

4.2.5 Thermal conductivity as a function of water content

Since the actual temperature influence on the thermal parameters does not seem very significant, thermal conductivity as a function of water content is only measured at ambient temperature. In a first series of experiments, sand-bentonite samples with different water content were prepared by placing them in exsiccators containing different salt solutions where they were stored until constant weight was reached (see next section for a more detailed description of the procedure). Afterwards the thermal parameters of the samples were measured using the Hotdisk system, in the same way as described before. After each measurement the actual water content of the sample was determined. The results are summarized in Tab. 4.3. Thermal conductivity as a function of water content is also shown in Fig. 4.11.

Tab. 4.3 Thermal parameters of granular sand-bentonite mixture at variable water content

Sample	Density	Thermal Conductivity	Thermal Diffusivity	Specific Heat	Temperature	Water Content
	ρ	K	κ	c	T	w_r
	kg/m ³	W/(m*K)	mm ² /s	MJ/(kg*K)	°C	%
12%	1508	0.305	0.278	$7.28 \cdot 10^{-4}$	25	1.14
31%	1541	0.362	0.280	$8.42 \cdot 10^{-4}$	25	2.70
54%	1545	0.370	0.288	$8.32 \cdot 10^{-4}$	25	3.75
70%	1528	0.364	0.247	$9.77 \cdot 10^{-4}$	25	4.63
90%	1539	0.411	0.314	$9.25 \cdot 10^{-4}$	25	5.27
100%	1477	0.433	0.306	$9.5 \cdot 10^{-4}$	25	9.07

As can be expected, there is an increase in all thermal parameters with increasing water content. The water content of 9.07 % reached at 100 % humidity in the exsiccator is, however, far from the value required for full saturation of the sample. From dry density and grain density of the sand-bentonite a porosity around 41 % can be calculated. A water content in the range of 27 % would be required for full saturation. The reason for this low water content is the low suction of the material which reaches a zero-value already around 28 % saturation (see next section).

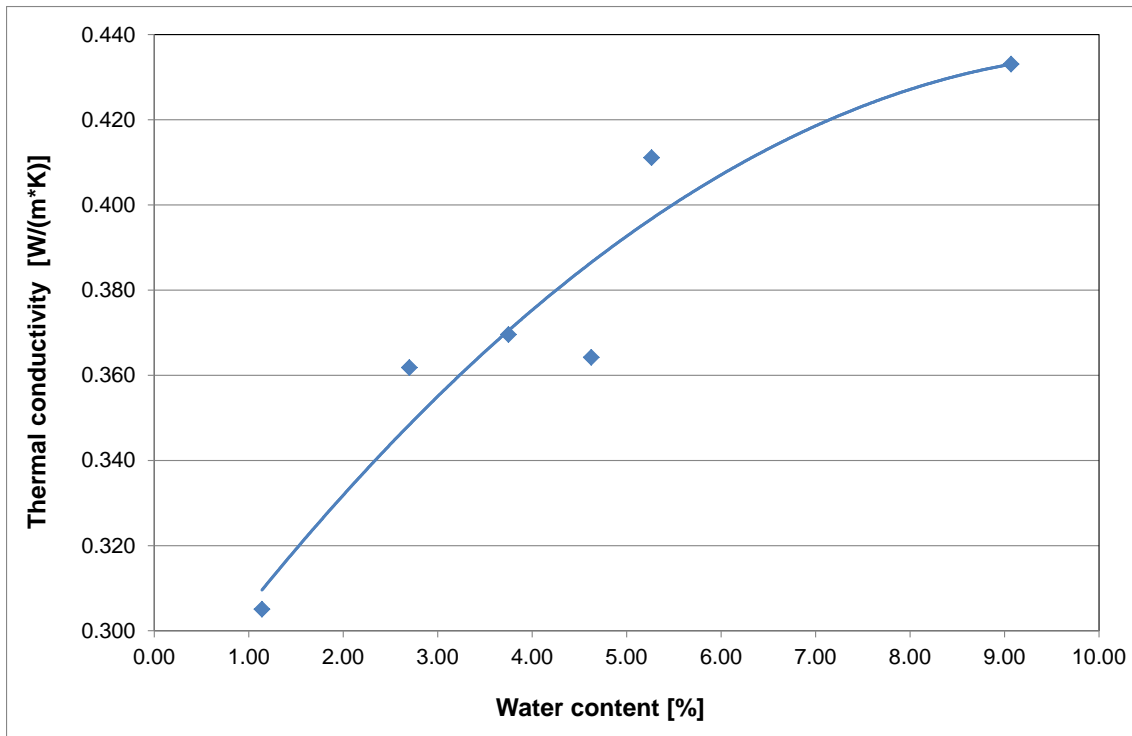


Fig. 4.11 Thermal conductivity of granular sand-bentonite as a function of temperature

For investigating thermal parameters of the sand-bentonite at higher saturation, samples have to be prepared differently. Instead of re-saturating them under a moist atmosphere, the water has to be added directly to the granular material. Respective samples have been prepared and currently measurements of the thermal parameters are underway. The results will be included in an update of this report.

4.3 Sample preparation and measurement of retention curve

For determination of the retention curve samples of sand-bentonite mixture were re-saturated in exsiccators (Fig. 4.12) containing different salt solutions in order to obtain different relative humidities in the atmosphere. Ten different solutions were used to obtain relative humidities between 6 % and 100 %. At each humidity value two samples were measured. The sample material was placed in open PVC cells with pierced bottom plates (Fig. 4.13) in order to get good contact between the humid air and the sample. To avoid sample material falling through the bottom holes, a filter paper was placed in the cell before emplacing the sand-bentonite. The cell dimensions are 48 mm diameter and 20 mm height.



Fig. 4.12 Exsiccators with sensors for temperature and humidity measurement



Fig. 4.13 PVC cell before placement of the sand-bentonite sample

The sample material was emplaced and flattened so that the surface was flush with the cell rim (Fig. 4.14). Emplacement density was chosen in a way that, considering the initial water content of the samples of 3.5 %, a dry density of $1.4 \text{ g/cm}^3 - 1.45 \text{ g/cm}^3$ was reached.



Fig. 4.14 Measurement cell filled with sand-bentonite sample

The samples were left in the exsiccators until a constant air humidity was reached; the minimum time for equilibration was seven days. Afterwards, the samples were removed from the exsiccators and the actual water content was determined by oven-drying at 105 °C following DIN 18121. From the water content the dry density was calculated. For calculation of the porosity the grain density of 2.546 g/cm³, measured with a gas pycnometer, was used. Porosity is calculated as

$$\Phi = 1 - \frac{\rho_d}{\rho_s}$$

Φ	Porosity of the mixture [-]
ρ_d	Dry density of the mixture [kg/m ³]
ρ_s	Grain density of the mixture [kg/m ³]

For plotting suction as a function of saturation the saturation is calculated as

$$S = \frac{\rho_d \cdot w}{\rho_w \cdot \Phi}$$

S	Degree of water saturation [-]
w	Water content [-]

ρ_d Dry density of the mixture [kg/m³]
 Φ Porosity of the mixture [-]

From the psychrometric law /FRE 93/ the suction is obtained from

$$s = \frac{R \cdot T \cdot \rho_w}{\omega_v} \cdot \ln(RH)$$

s Soil suction [kPa]
 R Universal gas constant (8.31432 J/(mol K))
 T Absolute temperature ($T = 273.16 + t$) [K]
 t Temperature [°C]
 ρ_w Density of water (998 kg/m³ at 20 °C)
 ω_v Molecular mass of water vapour (8.016 kg/kmol)
 RH Relative air humidity, [-]

In Tab. 4.4 the results of the measurements are summarized. Fig. 4.15 shows the corresponding suction/saturation diagram.

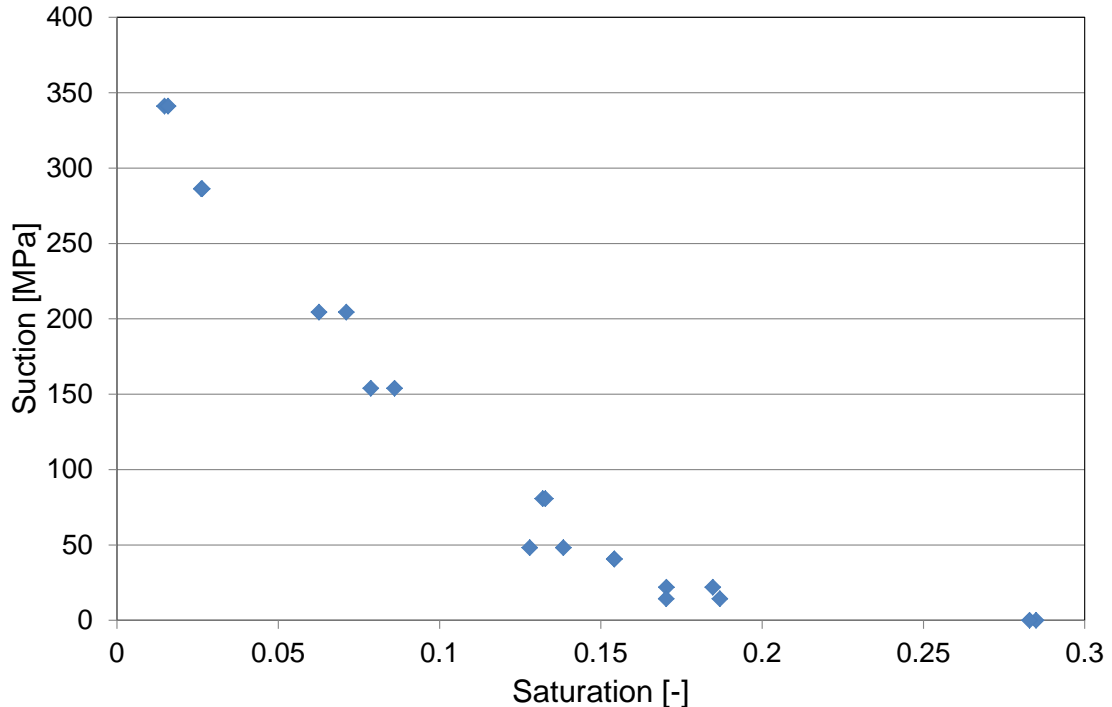


Fig. 4.15 Retention curve of granular sand-bentonite mixture

Tab. 4.4 Results of the retention curve measurements of granular sand-bentonite

Dry Density	Porosity	Water Content	Relative Air Humidity	Saturation	Suction
pd	Φ	w	RH	S	s
g/cm ³	-	-	-	-	MPa
1.437	0.436	0.0045	0.08	0.015	341.03
1.440	0.434	0.0048	0.08	0.016	341.03
1.382	0.457	0.0082	0.12	0.025	286.28
1.389	0.454	0.0082	0.12	0.025	286.28
1.411	0.446	0.0213	0.22	0.068	204.44
1.425	0.440	0.0193	0.22	0.063	204.44
1.421	0.442	0.0243	0.32	0.078	153.85
1.427	0.439	0.0265	0.32	0.086	153.85
1.438	0.435	0.0404	0.55	0.134	80.72
1.439	0.435	0.0406	0.55	0.135	80.72
1.431	0.438	0.0427	0.7	0.140	48.16
1.436	0.436	0.0400	0.7	0.132	48.16
1.446	0.432	0.0466	0.74	0.156	40.66
1.455	0.429	0.0463	0.74	0.157	40.66
1.468	0.423	0.0512	0.85	0.178	21.94
1.476	0.420	0.0554	0.85	0.195	21.94
1.470	0.423	0.0582	0.9	0.203	14.23
1.447	0.432	0.0518	0.9	0.174	14.23
1.445	0.433	0.0847	1	0.283	0
1.436	0.436	0.0849	1	0.280	0

The sand-bentonite mixture shows very low suction once a saturation above 15 % is reached. In fact, suction drops to zero at a saturation of only 28 %. This is a consequence of the rather low bentonite content and the high porosity. When the bentonite in the mixture is already saturated, there is still free pore space left in the material. This behaviour is also documented by the permeability properties of the material, as shown in the next section.

The suction of zero at 28 % saturation may be due to inaccuracy of the relative humidity measurement. In Fig. 4.16, the retention curve is plotted in a logarithmic scale, leaving out the value at 28 % porosity. The results seem to follow a straight line; the corresponding suction at 28 % porosity would be around 3 MPa and the humidity about 98 %.

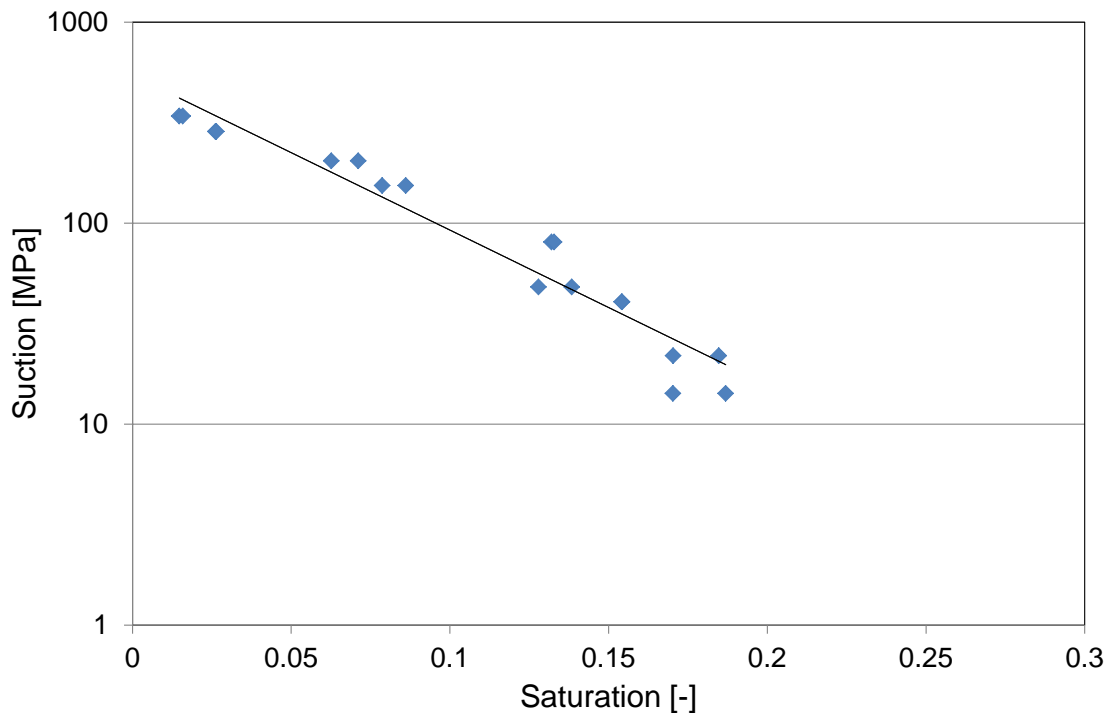


Fig. 4.16 Retention curve of granular sand-bentonite mixture, logarithmic scale

4.4 Permeability of granular sand-bentonite

The granular sand-bentonite material was placed in a cylindrical cell (Fig. 4.17). Emplacement density was 1504 kg/m^3 and the corresponding porosity 42.7 %. Permeability to gas was determined by nitrogen injection at five pressure steps between 0.111 MPa and 0.151 MPa (absolute pressure); the gas flow was measured using a burette. The permeability derived using Darcy's law was nearly identical for all pressure steps, with a value of $2.1 \cdot 10^{-12} \text{ m}^2$.

For measurement of the permeability to water the cell was placed horizontally (Fig. 4.17) and the sample was re-saturated with Pearson water very slowly at very low overpressure in mbar-range. The idea of the slow injection was to avoid flushing out of small particles. The following permeability measurement was performed at three differential pressures around 0.01 MPa. The resulting mean permeability value was $1.2 \cdot 10^{-13} \text{ m}^2$.

After finishing the experiment the sample was pressed out of the cell and dissected for water content measurement (Fig. 4.18). On the injection side the water content amounted to

29.9 %, decreasing slightly to 27.3 % on the outlet side. The mean water content was 28.3 %, meaning the material was completely saturated.

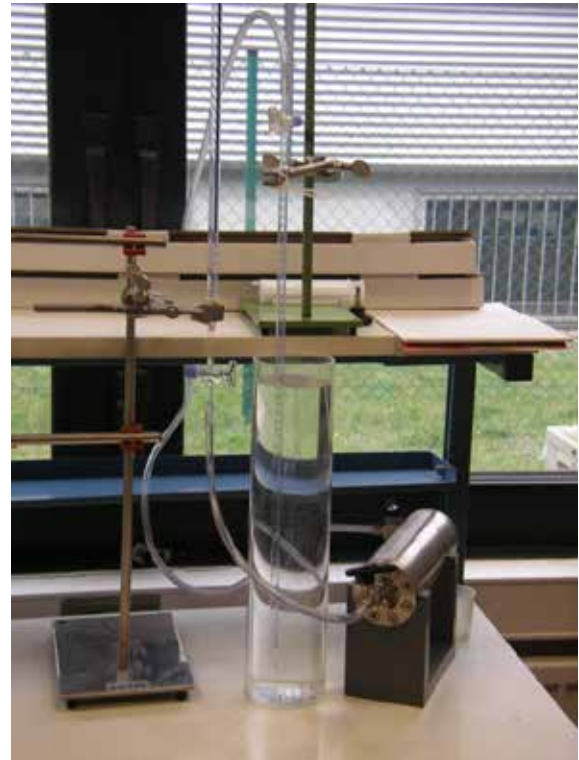


Fig. 4.17 System for measurement of sand-bentonite permeability to gas (left) and water (right)

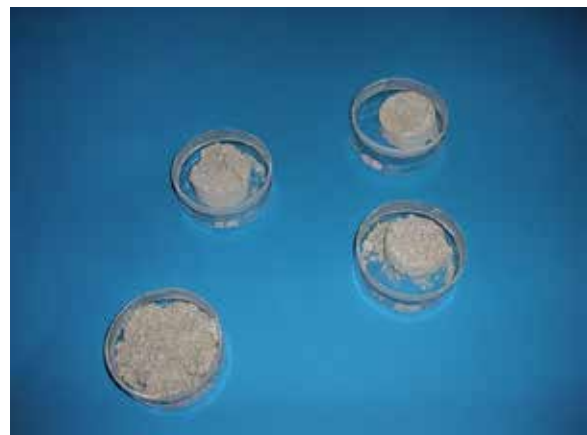


Fig. 4.18 Removal of saturated sand-bentonite from the cell

5 Measurements on granular bentonite

Preliminary measurements with the pure granular bentonite material were already performed in 2010. It has, however, to be noted that the sample density was higher than the actual density of the material emplaced in the HE-E. The material was emplaced in layers in Plexiglas containers. The sensor was located in the sample mid-plane, similar to the measurements with the SB material (Fig. 5.1). The material was investigated at as-delivered water content and after drying at 105 °C. The measurement results are compiled in Tab. 5.1.

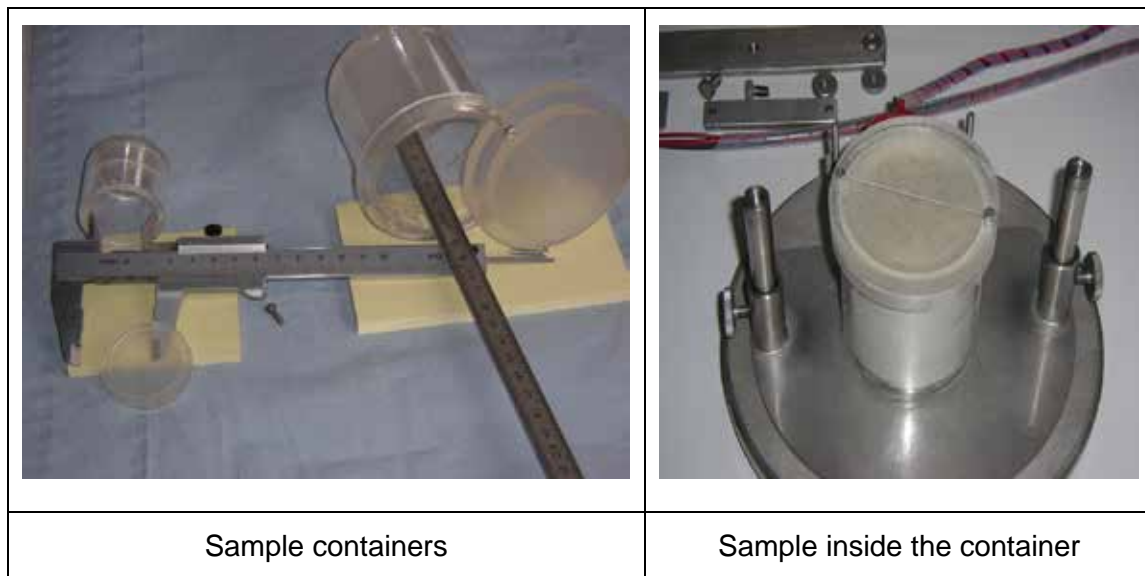


Fig. 5.1 Sample containers for the preliminary measurements on bentonite pellets

Tab. 5.1 Thermal parameters of granular bentonite buffer material, preliminary tests

Sample	Density	Thermal Conductivity	Thermal Diffusivity	Specific Heat	Temperature	Water Content
	ρ	K	K	c	T	w_r
	kg/m ³	W/(m*K)	mm ² /s	MJ/(kg*K)	°C	%
As-delivered material	1752	0.447	0.327	$7.82 \cdot 10^{-4}$	20°C	6.33
Dry material	1641	0.386	0.302	$7.79 \cdot 10^{-4}$	20°C	dry

In autumn 2011, a new measurement series was performed with the same buffer material, but with the new sample containers.

5.1 Sample preparation

In the laboratory of ETH Zürich the minimum (1470 – 1490 kg/m³) and maximum (1680 – 1700 kg/m³) emplacement densities for the granular bentonite material were determined /TEO 12/. For the measurement of the thermal parameters at the GRS lab it was tried to prepare samples with a bulk density below 1500 kg/m³. The preparation procedure was the same as for the sand-bentonite material (see Section 4.1).

It proved, however, impossible to prepare samples of this density with a sufficient coupling between the bentonite and the measuring probe. In contrast to the SB material, the pure granular bentonite has a much higher variation in grain size, which is the reason for this problem. Therefore, samples with a higher bulk density were used again for investigating the dependence of the thermal parameters on temperature. In the meantime, these problems were overcome. Currently measurements at relevant density and varying water content are performed; the results, however, are not yet available and will be reported in an update of this deliverable.

5.2 Determination of thermal parameters

The measurements were performed in the same way as with the sand-bentonite material. From the as-delivered granular bentonite an individual sample was prepared for each temperature step, while with the dried material the same sample could be used for all temperature steps, as discussed already in Section 4. The measurement results are shown in the Tables 5.2 and 5.3.

The density of the samples ranged around 1700 kg/m³. The water content of the as-delivered material ranged between 4.5 % and nearly 6 %, with a downward trend at higher temperature. It seems that, in contrast to the measurements with sand-bentonite, there was some evaporation during heating.

The water content of 5.91 % at ambient temperature is in good agreement with ETH measurements /TEO 12/ which resulted in 5.9 % - 6.0 %.

Tab. 5.2 Thermal parameters of the granular bentonite buffer material at as-delivered water content

Sample	Density	Thermal Conductivity	Thermal Diffusivity	Specific Heat	Temperature	Water Content
	ρ	K	κ	c	T	w_r
	kg/m ³	W/(m*K)	mm ² /s	MJ/(kg*K)	°C	%
granular bentonite buffer material	1667	0.338	0.366	5.54E-04	25	5.91
granular bentonite buffer material	1720	0.401	0.332	7.03E-04	40	5.62
granular bentonite buffer material	1687	0.415	0.316	7.78E-04	60	5.75
granular bentonite buffer material	1691	0.408	0.317	7.62E-04	80	5.42
granular bentonite buffer material	1726	0.435	0.315	8.01E-04	105	4.52

Tab. 5.3 Thermal parameters of the dried granular bentonite buffer material

Sample	Density	Thermal Conductivity	Thermal Diffusivity	Specific Heat	Temperature	Water Content
	ρ	K	κ	c	T	w_r
	kg/m ³	W/(m*K)	mm ² /s	MJ/(kg*K)	°C	%
granular bentonite buffer material; dry	1702	0.389	0.267	8.56E-04	25°C	dry
granular bentonite buffer material; dry	1702	0.403	0.278	8.52E-04	40°C	dry
granular bentonite buffer material; dry	1702	0.416	0.270	9.05E-04	60°C	dry
granular bentonite buffer material; dry	1702	0.427	0.266	9.46E-04	80°C	dry
granular bentonite buffer material; dry	1702	0.429	0.248	1.02E-03	105°C	dry

The thermal conductivity as a function of temperature is shown in Fig. 5.2. The curves for the dried and as-delivered material are very close, for two temperatures, the as-delivered material has an even lower thermal conductivity than the dried material. This is a clear hint that there are still major coupling problems. In the temperature range which is interesting for the HE-E, the thermal conductivity is in the same range (0.4 – 0.43 W/(m*K)) as for the granular sand-bentonite with a considerably lower density.

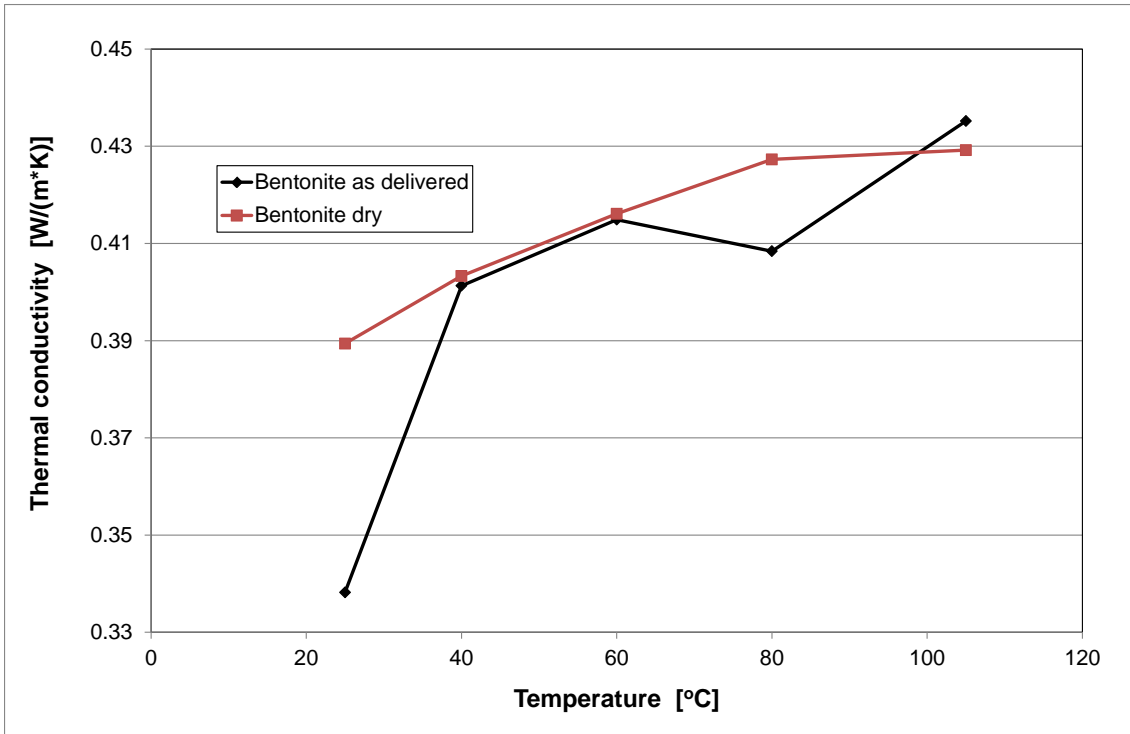


Fig. 5.2 Thermal conductivity of the dry (red) and as-delivered (black) bentonite samples as a function of temperature

Thermal diffusivity and specific heat are shown in Figs. 5.3 and 5.4, respectively. Specific heat is higher for the dried sample than for the as-delivered one, which can again only be explained by coupling problems, considering the fact the two of the as-delivered samples had an even higher density than the dry one. The specific heat of the as-delivered material of about $7 \cdot 10^{-4}$ MJ/(kg*K) - $8 \cdot 10^{-4}$ MJ/(kg*K) therefore is rather questionable, although it agrees with the earlier measurements.

Measurements on samples with a more realistic lower density are currently running.

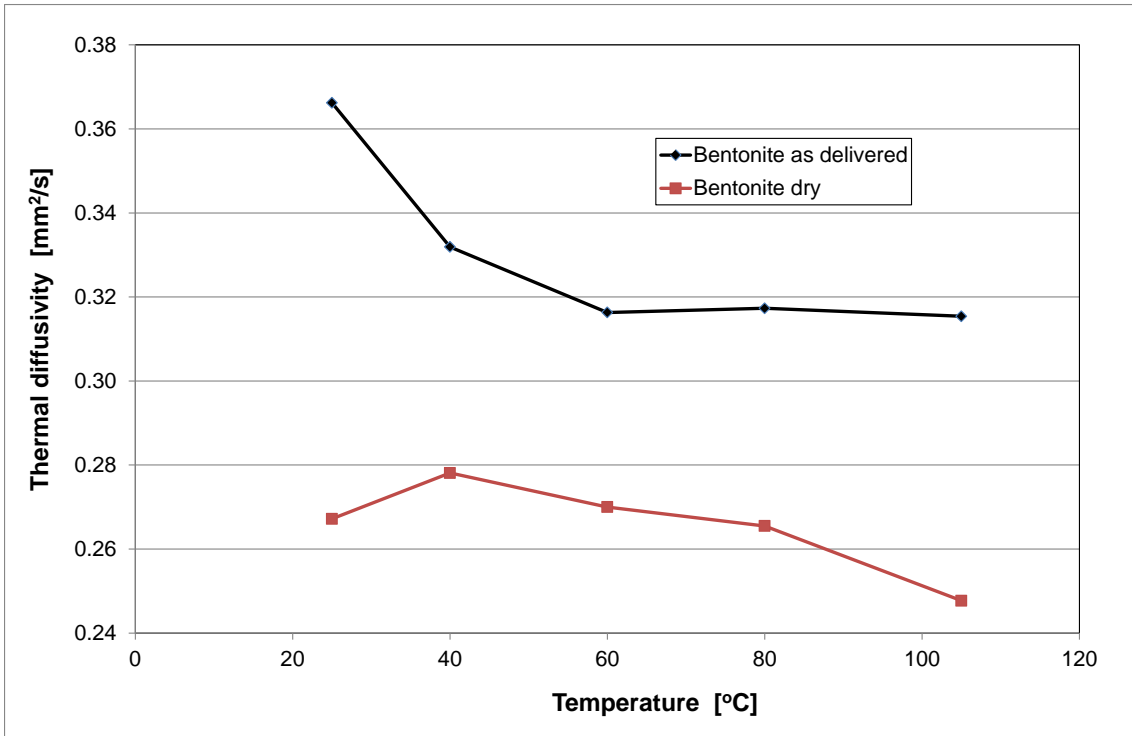


Fig. 5.3 Thermal diffusivity of the dry (red) and as-delivered (black) bentonite samples as a function of temperature

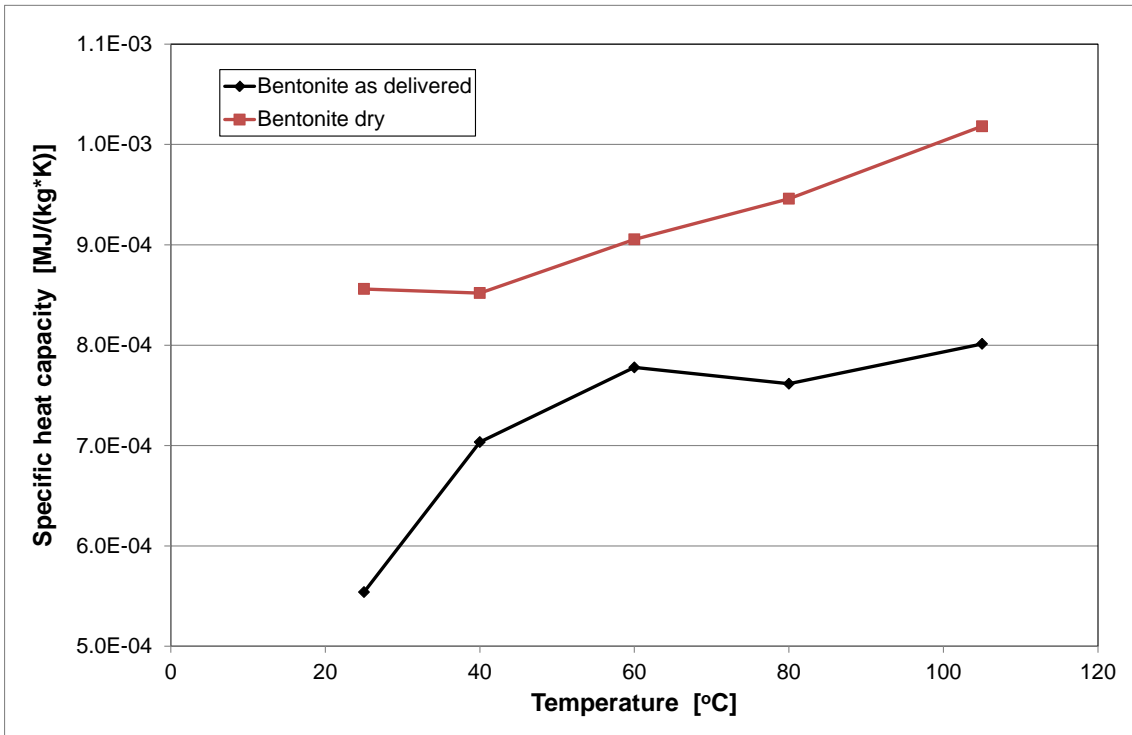


Fig. 5.4 Specific heat of the dry (red) and as-delivered (black) bentonite samples as a function of temperature

6 Conclusions and remaining work

Thermal parameters have been measured for the different buffer materials used in the HE-E: The bentonite blocks, the granular sand-bentonite mixture, and the pure granular bentonite. For all these materials, measurements were performed at ambient and elevated temperature at as-delivered water content. Measurements at increased water content have been performed for the sand-bentonite mixture, although not all of them are completed yet. For water contents above 10 %, the measurements are currently running. These and also measurements of pure granular bentonite at elevated water content will be reported in an update of this deliverable.

The effect of temperature on the thermal parameters appears not very significant in all materials, instead, assumed temperature effects more likely seem to be due to variations in water content or the quality of coupling between sample and sensor.

The results for the blocks and the sand-bentonite material, with the water content as delivered, can be used for modelling of the early phase of the HE-E. During the first years of heating, buffer re-saturation will not be significant. The temperature effect on the parameters is negligible. So, it seems reasonable to use constant values for thermal conductivity and specific heat, as long as saturation changes can be neglected. The suggested values are given here (Tab. 6.1).

Tab. 6.1 Thermal parameters of bentonite blocks and granular sand-bentonite at as-delivered water content

Material	Thermal Conductivity at as-delivered water content	Specific Heat at as-delivered water content
	K	c
	W/(m*K)	MJ/(kg*K)
Bentonite blocks	1.1	$1.8 \cdot 10^{-3}$
Granular sand-bentonite	0.4 – 0.43	$9 \cdot 10^{-4}$

With time, the different buffer materials will be re-saturated by pore water from the rock. Consequently, the dependence of the buffer materials' thermal parameters has to be quantified for longer term simulations. Measurements of the thermal parameters at different

water contents have partially been finished for the sand-bentonite material and will also be available soon for the pure granular bentonite.

In addition to the thermal parameters, measurements of the retention curve and the permeability were performed for the sand-bentonite mixture, since no respective data were available. While the results are valuable for modelling the HE-E, they also show that this material, in the actual configuration, is hardly suitable as buffer material. Because of constraints in handling, the material had to be installed in the HE-E without any compaction. The resulting high porosity led to insignificant swelling pressure and high permeability at full saturation. For use in a repository, the material would have to be changed, either by changing bentonite content and/or grain spectrum or by compaction.

7 References

- /FRE 93/ Fredlund, D.G., Rahardjo, H. (1993): Soil Mechanics for Unsaturated Soils, John Wiley&Sons, Inc.
- /HDT 07/ Instruction Manual, Hot Disk Thermal Constants Analyser, Hot Disk AB, 2007
- /PEB 10/ Long-term performance of Engineered Barrier Systems (PEBS), Annex I – “Description of Work”, Seventh Framework Programme, European Commission.
- /WIE 10/ Wieczorek, K., Miehe, R. (2011): Measurement of Thermal Parameters of the HE-E Buffer Materials, Deliverable D2.2-5 of the PEBS project.
- /TEO 12/ Teodori, S.-P., Gaus, I. (Ed.) (2012): Report of the construction of the HE-E experiment, Deliverable D2.2-3 of the PEBS project.

8 List of figures

Fig. 1.1	Overview of the HE-E configuration.....	1
Fig. 2.1	Principle measurement configuration /HDT 07/	3
Fig. 2.2	Sensors for the Hotdisk analyser.....	4
Fig. 3.1	Grooved upper bentonite block.....	6
Fig. 3.2	Sample pair STU1/STU2.....	7
Fig. 3.3	Sample pair in the drying oven (the clamping device is used to assure coupling of sensor to the bentonite).....	8
Fig. 3.4	Thermal conductivity of the different samples from the bentonite blocks as a function of temperature.....	11
Fig. 3.5	Thermal conductivity of the different samples from the bentonite blocks as a function of water content.....	12
Fig. 3.6	Thermal diffusivity of the different samples from the bentonite blocks as a function of temperature.....	13
Fig. 3.7	Specific heat of the different samples from the bentonite blocks as a function of temperature	14
Fig. 4.1	Sample container for SB samples	15
Fig. 4.2	Sample container with SB layer, in red: measurement sensor	16
Fig. 4.3	Inserting the sensor into the sample container	16
Fig. 4.4	Sensor and SB layer inside the sample container.....	17
Fig. 4.5	Emplacement of second SB layer into the sample container	17
Fig. 4.6	Filled sample container before closing.....	18

Fig. 4.7	Prepared sample in the oven.....	18
Fig. 4.8	Thermal conductivity of the dry (red) and as-delivered (black) SB samples as a function of temperature.....	21
Fig. 4.9	Thermal diffusivity of the dry (red) and as-delivered (black) SB samples as a function of temperature.....	22
Fig. 4.10	Specific heat of the dry (red) and as-delivered (black) SB samples as a function of temperature	22
Fig. 4.11	Thermal conductivity of granular sand-bentonite as a function of temperature ..	24
Fig. 4.12	Exsiccators with sensors for temperature and humidity measurement.....	25
Fig. 4.13	PVC cell before emplacement of the sand-bentonite sample.....	25
Fig. 4.14	Measurement cell filled with sand-bentonite sample.....	26
Fig. 4.15	Retention curve of granular sand-bentonite mixture	27
Fig. 4.16	Retention curve of granular sand-bentonite mixture, logarithmic scale	29
Fig. 4.17	System for measurement of sand-bentonite permeability to gas (left) and water (right).....	30
Fig. 4.18	Removal of saturated sand-bentonite from the cell.....	30
Fig. 5.1	Sample containers for the preliminary measurements on bentonite pellets	31
Fig. 5.2	Thermal conductivity of the dry (red) and as-delivered (black) bentonite samples as a function of temperature.....	34
Fig. 5.3	Thermal diffusivity of the dry (red) and as-delivered (black) bentonite samples as a function of temperature.....	35
Fig. 5.4	Specific heat of the dry (red) and as-delivered (black) bentonite samples as a function of temperature.....	35

9 List of tables

Tab. 3.1	Thermal parameters of the upper block, as delivered	10
Tab. 3.2	Thermal parameters of the lower block, as delivered.....	10
Tab. 3.3	Thermal parameters of the upper and lower block samples after drying	11
Tab. 4.1	Thermal parameters of the granular sand-bentonite buffer material at as-delivered water content	19
Tab. 4.2	Thermal parameters of the dried granular sand-bentonite buffer material.....	20
Tab. 4.3	Thermal parameters of granular sand-bentonite mixture at variable water content	23
Tab. 4.4	Results of the retention curve measurements of granular sand-bentonite	28
Tab. 5.1	Thermal parameters of granular bentonite buffer material, preliminary tests.....	31
Tab. 5.2	Thermal parameters of the granular bentonite buffer material at as-delivered water content	33
Tab. 5.3	Thermal parameters of the dried granular bentonite buffer material	33
Tab. 6.1	Thermal parameters of bentonite blocks and granular sand-bentonite at as-delivered water content	36